12th AIAA/ISSMO Multidisciplinary Analysis and Optimization Conference
10 - 12 September 2008, Victoria, British Columbia Canada

AIAA 2008-5931

Continuous Sensitivity Analysis of Fluid-Structure Interaction Problems using Least-Squares Finite Elements

Douglas P. Wickert[1], Robert A. Canfield[2]
Air Force Institute of Technology, Wright-Patterson AFB, OH, 45433, USA

J. N. Reddy[3]
Texas A&M University, College Station, Texas 77843-3123, USA

A least-squares continuous sensitivity analysis method is developed for fluid-structure interaction problems to support computationally efficient analysis and optimization of aeroelastic design problems. The continuous sensitivity system equations and sensitivity boundary conditions are derived and the problem is posed in first-order form. A least-squares finite element solution of the coupled fluid-structure physics is then used to determine the sensitivity boundary conditions. The least-squares finite element method permits a simultaneous solution of the fluid-structure system and the mesh deformation problem within a single numerical framework. A least-squares finite element solution of the linear continuous sensitivity equations is then used to produce computationally efficient design parameter gradient calculations without needing to derive and code the problematic mesh sensitivities. An example nonlinear fluid-structure interaction problem is solved. Continuous sensitivity results for both the local and total material derivatives are presented and compared to gradients obtained by finite-difference methods.

I. Introduction

Ongoing research efforts are seeking new methods for effective and computationally efficient analysis to support large-scale design optimization of elastic aircraft structures. One aspect of these efforts are high-fidelity, nonlinear, aeroelastic models suitable for aircraft gust response [1]. Another aspect of the research efforts involves creating effective surrogate models for efficient large-scale optimization [2]. Aeroelasticity is a challenging science, dealing with the interaction of two very different domains governed by disparate physics. Nonlinear aspects of both the fluid and structural domains can make accurate calculations of the interaction problematic, not the least due to the substantial computational expenses involved. Since optimization and inverse design methods typically require some measure of the change of an objective function or performance parameter to variations in design parameters, optimization of aeroelastic problems, which are themselves computationally intensive, challenging, and expensive to solve, can be outright formidable. Thus, this subject represents a prime frontier for basic research

Design sensitivity methods can be grouped [3] into numerical approximate methods or analytic and semi-analytic methods as indicated in Figure 1 . Numerical approaches, e.g. finite difference, are expensive in that they require multiple solutions of the problem. Proper determination of the design parameter perturbation step size--trading off truncation error and round-off error--can also be challenging. The analytic and semi-analytic methods

The views expressed in this paper are those of the author and do not reflect the official policy or position of the United States Air Force, Department of Defense, or the United States Government.

[1] PhD Candidate, Department of Aeronautical and Astronautical Engineering, 2950 Hobson Way, Wright-Patterson AFB, OH 45433-7765, AIAA Student Member.

[2] Associate Professor, Department of Aeronautical and Astronautical Engineering, 2950 Hobson Way, Wright-Patterson AFB, OH 45433-7765, AIAA Associate Fellow.

[3] Distinguished Professor, Department of Mechanical Engineering;jnreddy@shakti.tamu.edu. AIAA Fellow.

can be further classified as either discrete or continuous, the difference depending on the order of the discretization and differentiation steps [4]. The most common approach is to discretize the system first and calculate sensitivities by either direct or adjoint methods. For shape sensitivity problems, the mesh sensitivity must also be calculated which can be problematic. In continuous sensitivity analysis, the design parameter gradients are calculated from the continuous equations yielding a system of differential equations for the sensitivity variables, which are, in turn, discretized [5, 6]. Thus, the continuous sensitivity method for gradient calculation can efficiently produce design parameter gradients needed by most optimization algorithms without needing to invert the mesh Jacobian. The resulting sensitivity system of equations is always linear, even for nonlinear systems, which is particularly attractive for the nonlinear aeroelastic problems considered here.

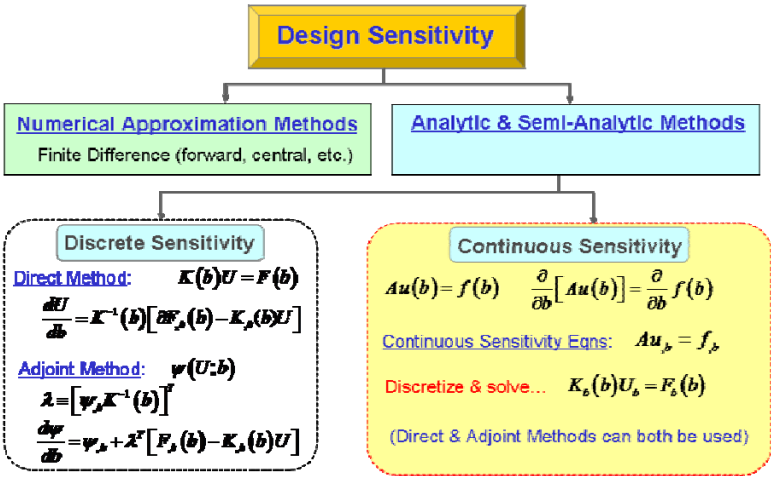

Figure 1 Classification and methods of design sensitivity analysis

Overall, shape sensitivity and optimization methods are more mature for structural problems [7] than they are for fluid problems, but they have not typically employed continuous sensitivity methods [4, 8]. Although there now exists an extensive body of literature involving the application of continuous sensitivity methods to fluid dynamics problems, the application to structural elasticity problems is complicated by the nature of the sensitivity of the stress tensor [9, 10]. Shape sensitivity methods have been applied to fluid-structure interaction problems in several studies [11], but the use of continuous sensitivity methods in aeroelasticity is far more limited and recent [12][13][14]. To our knowledge, this is the first effort to use least-squares finite element (LSFEM) methods to solve both the fully-coupled fluid-structure interaction physics and the sensitivity equations with the same computational framework. We also make a clear distinction between the total material and local derivatives for the continuous sensitivity calculations.

Currently, the most common approach for solving fluid-structure interaction (FSI) problems uses different theoretical formulations and numerical methods to solve the fluid and structure problems separately, a method that can be fraught with convergence issues and inaccurate solutions when the method does converge [15, 16]. A more significant drawback is that when applied to (numerical approximate) sensitivity applications, the iterative nature of the segregated strategy may require multiple computationally expensive cycles for every variation of an individual design variable. If scaled to hundreds or thousands of design variables, the segregated method is computationally intractable for numerical approximate methods. Alternative FSI solution strategies casts the coupled fluid, structure, and mesh deformation systems as a single monolithic or fully-coupled fluid-structure-mesh formulation [17-19]. This approach generally gives faster convergence [20], though the memory requirements are substantially greater since the fluid, structure, and mesh degrees of freedom must be treated and solved simultaneously. As overall computer performance improves and the expense of large memory approaches decreases, the trend in aeroelastic computational methods is towards full coupling of the fluid-structure-mesh systems [21, 22], though there are still several open research questions regarding the proper weighting between the different physics and interface between the separate fluid and structure domains. By employing continuous sensitivity methods below for a segregated FSI solution, we avoid the numerical shortcomings of the segregated approach without having to determine the proper domain and interface weights for a monolithic solution.

A least-squares finite element method (LSFEM) formulation for the FSI problem is promising in that it provides a consistent approach with the same numerical framework for the simultaneous solution of the fully-coupled fluid, structure , and accompanying mesh deformation problems [23][24]. The LSFEM method is in the class of weighted residual variational solutions to partial differential equations and has seen a renaissance of interest in the last several years: [24-33] are representative of the range of applications to both fluid and structural problems. A LSFEM approach seeks to minimize the L^2 norm of the residual error of the governing differential equations. Least-squares methods for time-dependent and nonlinear problems are well-established in the literature [26], and appear applicable to analysis of transient, nonlinear gust response. Gust response loads are of particular interest as they have been identified as the critical load condition for several proposed aerospace applications, including a next-generation, long-endurance vehicle designed for persistent intelligence, surveillance, and reconnaissance missions [34, 35]. The sensitivity to transient gust loads will be considered in future work.

This paper begins with a description of the continuous sensitivity method. The formulation of the least-squares finite element solution for the fluid, structure, and interface system is then described. The next section solves an example FSI problem using the least-squares continuous sensitivity method. The continuous sensitivity results for both the local and total material derivatives are presented and compared to finite difference derived gradients.

II. Continuous Sensitivity Equations

Consider the following general boundary value system defined in a domain Ω with a boundary Γ for which we seek a solution $\mathbf{u}$

$$\mathbf{A}\mathbf{u} = \mathbf{f} \text{ in } \Omega \tag{1}$$

$$\mathbf{B}\mathbf{u} = \mathbf{g} \text{ on } \Gamma \tag{2}$$

$\mathbf{A}$ is a first-order time-space differential operator given by

$$\mathbf{A} = \mathbf{A}_t \frac{\partial}{\partial t} + \sum_{i=1}^{\dim} \mathbf{A}_i \frac{\partial}{\partial x_i} + \mathbf{A}_0 \tag{3}$$

and, $\mathbf{B}$, the boundary condition operator, has the form

$$\mathbf{B} = \mathbf{B}_t \frac{\partial}{\partial t} + \mathbf{B}_1 \frac{\partial}{\partial \xi_i} + \mathbf{B}_0 \tag{4}$$

where ξ is a coordinate that parameterizes the boundary (e.g. arc length). The forward difference approach for calculating the sensitivity of the solution with respect a design parameter, b, is

$$\frac{\partial \mathbf{u}}{\partial b} \approx \frac{\mathbf{u}(b+\delta b) - \mathbf{u}(b)}{\delta b} \tag{5}$$

Besides the computational expensive involved in solving the system twice, a challenge in finite difference method is in determining the optimum step size. Large steps are dominated by truncation error (which can be significant if the system is nonlinear and exhibits sensitive depedance on the boundary conditions) and small steps are dominated by numerical round-off error.

The continuous sensitivity method avoids the numerical shortcomings of finite difference methods by differentiating the field equations (1)-(2) to yield a governing continuous system of equations for the desired sensitivity variables. For example, differentiating (1) with respect to the design parameter, b, yields

$$\frac{\partial}{\partial b}\left[A_t \mathbf{u}_{,t} + A_0 \mathbf{u} + A_1 \mathbf{u}_{,x} + A_2 \mathbf{u}_{,y} \right] = \frac{\partial}{\partial b}\left[\mathbf{f} \right] \tag{6}$$

which expands as

$$A_{t,b} \frac{\partial \mathbf{u}}{\partial t} + A_{0,b}\mathbf{u} + A_{1,b}\mathbf{u}_{,x} + A_{2,b}\mathbf{u}_{,y} + A_t \frac{\partial}{\partial b}\frac{\partial \mathbf{u}}{\partial t} + A_0 \frac{\partial}{\partial b}\mathbf{u} + A_1 \frac{\partial}{\partial b}\frac{\partial \mathbf{u}}{\partial x} + A_2 \frac{\partial}{\partial b}\frac{\partial \mathbf{u}}{\partial y} = \frac{\partial \mathbf{f}}{\partial b} \tag{7}$$

Since the spatial-temporal derivatives are independent operations from the sensitivity derivative, the order of differentiation may be reversed. Defining the sensitivity variables as

$$ {}^{b}\mathbf{u} \equiv \frac{\partial}{\partial b}\mathbf{u} \tag{8} $$

and collecting appropriate terms yields the continuous sensitivity system

$$ {}^{b}\mathbf{A}\left({}^{b}\mathbf{u}\right) \equiv {}^{b}A_t\left({}^{b}\mathbf{u}_{,t}\right) + {}^{b}A_0^*\left({}^{b}\mathbf{u}\right) + {}^{b}A_1^*\left({}^{b}\mathbf{u}_{,x}\right) + {}^{b}A_2^*\left({}^{b}\mathbf{u}_{,y}\right) = {}^{b}\mathbf{f} \tag{9} $$

where ${}^{b}\mathbf{f} \equiv \partial/\partial b\,\mathbf{f}$ and ${}^{b}\mathbf{A}$ is the sensitivity system time-space differential operator. For linear systems with b representing a boundary shape parameter, the original system time-space differential operator, $\mathbf{A}$, is not a function of b. Thus the first four terms in (7) vanish and the component CSE operators, ${}^{b}A$, are identical to the original system operators, A. For nonlinear systems, the nonlinear components of the original system change ${}^{b}A_0$, but ${}^{b}A_1 = A_1$ and ${}^{b}A_2 = A_2$. The continuous sensitivity system is always linear, even when the original system is nonlinear. The continuous sensitivity system is thus simply another system of differential equations which together with the appropriate boundary data represents a well-posed boundary value problem which may be solved by any of a wide variety of numerical approaches. It is convenient in many cases to use the same numerical method/framework to solve the sensitivity system as was used to solve the original system.

The sensitivity equation boundary conditions specify how the sensitivity variables behave on the boundary of the domain. Thus, analogous to the approach used above, the sensitivity of boundary operator system, (2), may be written as a CSE system

$$ {}^{b}\mathbf{B}\left({}^{b}\mathbf{u}\right) = {}^{b}\mathbf{g} \quad \text{on } \Gamma \tag{10} $$

For shape variation problems, there are two ways in which boundary values for a scalar or vector field variable (considered component-wise), u, may change on the boundary. First, the boundary condition of the original problem may be altered by a change in the design parameter. Second, the design parameter may alter the shape of the boundary and domain and thus the value of the field variable. These are related through the concept of the material derivative

$$ \left.\frac{Du}{Db}\right|_{\mathbf{X}} = \left.\frac{\partial u}{\partial b}\right|_{\mathbf{x}} + \nabla u \cdot \left.\frac{\partial \mathbf{x}}{\partial b}\right|_{\mathbf{X}} \tag{11} $$

where $\mathbf{X}$ denotes a material coordinate and $\mathbf{x}$ denotes a spatial coordinate (Eulerian description). Thus the total derivative of u with respect to b at a material point $\mathbf{X}_0$ consists of the local derivative of u with respect to parameter b and a transport term which accounts for how the material point $\mathbf{X_0}$ changes character in spatial coordinates as the design parameter b varies. If u is a vector quantity, then the gradient operation and dot product in the advection term is carried out row-wise. The desired sensitivity variable boundary condition for a scalar or vector quantity is thus

$$ {}^{b}\mathbf{u}\Big|_{\Gamma} \equiv \left.\frac{\partial \mathbf{u}}{\partial b}\right|_{\mathbf{X}=\Gamma} = \left.\frac{D\mathbf{u}}{Db}\right|_{\Gamma} - \nabla \mathbf{u} \cdot \frac{\partial \mathbf{x}_{\Gamma(b)}}{\partial b} \tag{12} $$

The first term on the right hand side accounts for how the boundary conditions for the problem change with respect to the design parameter. In most cases, this term is zero. That is, the boundary condition does not change as the shape changes. The advection term uses the gradient of the solution. In a finite element solution, this expression comes from the gradient of the shape functions applied to the finite element solution.

If the dependent variable is a tensor, as in the case of the fluid or structure stress tensor, then the more complicated upper convected derivative or Oldroyd derivative must be used in place of (11)

$$ \mathbf{S}^{\nabla} = \frac{D}{Db}\mathbf{S} - \left(\nabla \frac{\partial \mathbf{x}}{\partial b}\right)^{T} \cdot \mathbf{S} - \mathbf{S} \cdot \left(\nabla \frac{\partial \mathbf{x}}{\partial b}\right) \tag{13} $$

where $\nabla \partial \mathbf{x}/\partial b$ is the tensor of design parameter velocities. Equation (13) is equivalent to the stress tensor sensitivity expressed in terms normal and tangential surface tractions derived in a much different manner by Dems and Haftka [9]

$$ {}^{b}\sigma_{ij}^{s} n_j = \frac{DT_i}{Db} - \sigma_{ij,k} n_j \frac{\partial \phi_k}{\partial b} - \sigma_{ij}\left(n_j n_l - \delta_{jl}\right) n_k \left[\frac{\partial \phi_k}{\partial b}\right]_{,l} \tag{14} $$

where tensor index notation has been used, T_i are the components of the surface traction vector, n_i are the components of the unit normal/tangential vector, δ is the delta function, and ϕ is the transformation field that maps material coordinates of the domain as a function of the design parameter. Formal comparison and expansion of (13) and (14) is considered in future work[36].

III. Fluid-Structure Interaction Governing Equations

A. Incompressible, Inviscid, Irrotational Fluid (Potential Flow)

An incompressible, inviscid fluid is governed by the continuity equation

$$ \nabla \cdot \mathbf{u} = 0 \quad \text{in } \Omega^f \tag{15} $$

and the momentum equation

$$ \frac{\partial \mathbf{u}}{\partial t} + \left(\mathbf{u} \cdot \nabla\right)\mathbf{u} + \nabla p = \mathbf{f} \quad \text{in } \Omega^f \tag{16} $$

where $\mathbf{u}$ is the fluid velocity vector, p is pressure, and $\mathbf{f}$ is the body force. Under steady conditions with no body forces, the momentum equation reduces to Bernoulli's equation

$$ p = p_0 + \tfrac{1}{2}\rho \mathbf{u} \cdot \mathbf{u} \quad \text{in } \Omega^f \tag{17} $$

For irrotational flow, the vorticity, $\boldsymbol{\omega} \equiv \nabla \times \mathbf{u}$, is zero. Thus

$$ \nabla \times \mathbf{u} = 0 \quad \text{in } \Omega^f \tag{18} $$

In 2-D, (15) and (18) become

$$ u_{,x} + v_{,y} = 0 \tag{19} $$

and

$$ -u_{,y} + v_{,x} = 0 \tag{20} $$

which are also the governing equations for a potential flow field governed by Laplace's equation. The matrix operator form with $\mathbf{u}^f = \{u \quad v\}^T$ is

$$ A_0^f \mathbf{u} + A_1^f \mathbf{u}_{,x} + A_2^f \mathbf{u}_{,y} = \mathbf{f} \tag{21} $$

where

$$ A_0^f = \begin{bmatrix} 0 & 0 \\ 0 & 0 \end{bmatrix}, \quad A_1^f = \begin{bmatrix} 1 & 0 \\ 0 & 1 \end{bmatrix}, \quad A_2^f = \begin{bmatrix} 0 & 1 \\ -1 & 0 \end{bmatrix}, \quad \mathbf{f}^f = \begin{bmatrix} 0 \\ 0 \end{bmatrix} \tag{22} $$

The *f* superscripts are introduced to denote fluid domain variables. Note that pressure is determined using the fluid velocity solution along with (17).

B. Euler-Bernoulli Beam

The governing equation for the deflection, *v,* of an Euler-Bernoulli beam subject to a transverse load per unit length, p_y is [37]

$$\rho \frac{\partial^2 v}{\partial t^2} + \frac{\partial^2}{\partial x^2}\left(EI \frac{\partial^2 v}{\partial x^2} \right) = p_y \tag{23}$$

Considering a steady-state system and introducing

$$\theta = v_{,x} \tag{24}$$

$$M_z = EIv_{,xx} = \theta_{,x} \tag{25}$$

$$V_y = -M_{z,x} \tag{26}$$

where θ is the beam slope, M_z is the internal bending moment, and V_y is the internal shear force allows decomposition of (23) into first-order matrix operator form

$$A_t^s \mathbf{u}_{,tt}^s + A_0^s \mathbf{u}^s + A_1^s \mathbf{u}_{,x}^s = \mathbf{f}^s \tag{27}$$

where $\mathbf{u}^s = \begin{bmatrix} v & \theta & M_z & V_y \end{bmatrix}^T$ and the matrix operators are

$$A_0^s = \begin{bmatrix} 0 & 1 & 0 & 0 \\ 0 & 0 & 1/EI & 0 \\ 0 & 0 & 0 & -1 \\ 0 & 0 & 0 & 0 \end{bmatrix} \quad A_1^s = \begin{bmatrix} -1 & 0 & 0 & 0 \\ 0 & -1 & 0 & 0 \\ 0 & 0 & -1 & 0 \\ 0 & 0 & 0 & -1 \end{bmatrix} \quad \mathbf{f}^s = \begin{bmatrix} 0 \\ 0 \\ 0 \\ p_y \end{bmatrix} \tag{28}$$

IV. Least-Squares Finite Element Method

The square of the system weighted residuals for (1) and (2) defines a functional

$$J(\mathbf{u};\mathbf{f},\mathbf{g}) = \alpha \left\| \mathbf{Au} - \mathbf{f} \right\|_\Omega^2 + (1-\alpha) \left\| \mathbf{Bu} - \mathbf{g} \right\|_\Gamma^2 \tag{29}$$

where

$$\left\| \cdot \right\|_\Omega^2 \equiv \int_\Omega (\cdot)^2 d\Omega \geq 0 \quad \text{and} \quad \left\| \cdot \right\|_\Gamma^2 \equiv \int_\Gamma (\cdot)^2 d\Gamma \geq 0 \tag{30}$$

are the L^2 norms and $0 < \alpha < 1$ is the residual weighting factor. A necessary condition for **u** to minimize (29) is that the first variation of (29) vanishes at **u** [38]. This yields an equivalent bilinear/linear inner product form [39] for the boundary value system (1)-(2)

$$B(\mathbf{u},\mathbf{v}) = l(\mathbf{f},\mathbf{v}) \quad \forall \mathbf{v} \in \mathbf{V} \tag{31}$$

where

$$\begin{aligned} B_\Omega(\mathbf{u},\mathbf{v}) &\equiv (\mathbf{Au},\mathbf{Av}) \\ l_\Omega(\mathbf{f},\mathbf{v}) &\equiv (\mathbf{f},\mathbf{Av}) \end{aligned} \tag{32}$$

and

$$\begin{aligned} B_\Gamma(\mathbf{u},\mathbf{v}) &\equiv (\mathbf{Bu},\mathbf{Bv}) \\ l_\Gamma(\mathbf{g},\mathbf{v}) &\equiv (\mathbf{g},\mathbf{Bv}) \end{aligned} \tag{33}$$

For most of our present effort, $\mathbf{V} \subseteq L_2(\Omega)$, the *Lebesque* space consisting of square-integrable functions; or $\mathbf{V} \subseteq H^1(\Omega)$, the basic *Sobolev* space (a *Hilbert* space with first-order derivatives defined) [40]. The domain will be partitioned into finite elements and in each element, we approximate the solution **u** by

$$\mathbf{u} \approx \mathbf{u}_h^e = \sum_{j=1}^{n_{dof}^e} \psi_j \left[u_1 \ldots u_{n_{nodes}} \quad a_1 \ldots a_{n_a} \quad b_1 \ldots b_{n_a} \right]^T \tag{34}$$

where ψ_j are shape functions [41]. The element degrees of freedom, $n_{dof}^e = n_{nodes} + n_a + n_b$, consist of the element nodal values, $u_1 \ldots u_{n_{nodes}}$, the edge coefficients, $a_1 \ldots a_{n_a}$, and the interior (bubble) mode coefficients, $b_1 \ldots b_{n_a}$. This set of degrees of freedom assumes a higher-order hierarchal expansion of shape functions [42]. In what follows, we adopt Szabo's quadrilateral shape function expansion basis [43] which is a serendipity expansion built of kernel functions constructed from Legendre polynomials. Another commonly used expansion consisting of complete polynomials is based on a tensor product expansion of Legendre polynomials in two dimensions [44].

Substituting (34) into (32) yields n_{dof}^e algebraic equations which are evaluated to determine the element stiffness matrix and equivalent force vector

$$\mathbf{K}^e = \int_{\Omega^e} \left(\mathbf{A}\psi_1, \ldots, \mathbf{A}\psi_{n_{dof}^e} \right)^T \left(\mathbf{A}\psi_1, \ldots, \mathbf{A}\psi_{n_{dof}^e} \right) d\Omega \tag{35}$$

$$\mathbf{F}^e = \int_{\Omega^e} \left(\mathbf{A}\psi_1, \ldots, \mathbf{A}\psi_{n_{dof}^e} \right)^T \mathbf{f} \, d\Omega \tag{36}$$

$$\mathbf{K}_\Gamma^e = \int_{\Gamma^e} \left(\mathbf{B}\psi_1, \ldots, \mathbf{B}\psi_{n_{dof}^e} \right)^T \left(\mathbf{B}\psi_1, \ldots, \mathbf{B}\psi_{n_{dof}^e} \right) d\Gamma \tag{37}$$

$$\mathbf{G}^e = \int_{\Gamma^e} \left(\mathbf{B}\psi_1, \ldots, \mathbf{B}\psi_{n_{dof}^e} \right)^T \mathbf{g} \, d\Gamma \tag{38}$$

The element stiffness and load vectors are assembled into a global system based on a global dof table. The global system then has the form

$$\left[\alpha \mathbf{K} + (1-\alpha) \mathbf{K}_\Gamma \right] \mathbf{u} = \alpha \mathbf{F} + (1-\alpha) \mathbf{G} \tag{39}$$

V. FSI and CSE Example Problem

The example FSI problem in Figure 2 is a NACA 0012 airfoil shape is mounted on a flexible sting. The sting is modeled as 1D Euler-Bernoulli beam. The entire system is immersed in an incompressible, inviscid, irrotational fluid. At a positive angle of attack, the airfoil generates lift, deflecting the beam in the fluid resulting in an increased angle of attack. An iterative sequential solution scheme is used for both the fluid flow solution and the beam deflection and is repeated until the beam deflection converges to a steady-state value.

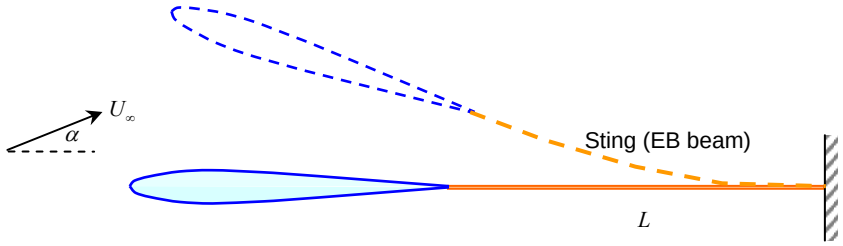

Figure 2 Flexible sting mounted airfoil

The FSI problem boundary conditions are given in Figure 3 and Table 1 The LSFEM FSI solution is given in Figure 3 using a fourth order expansion basis for both the fluid and structure domains.

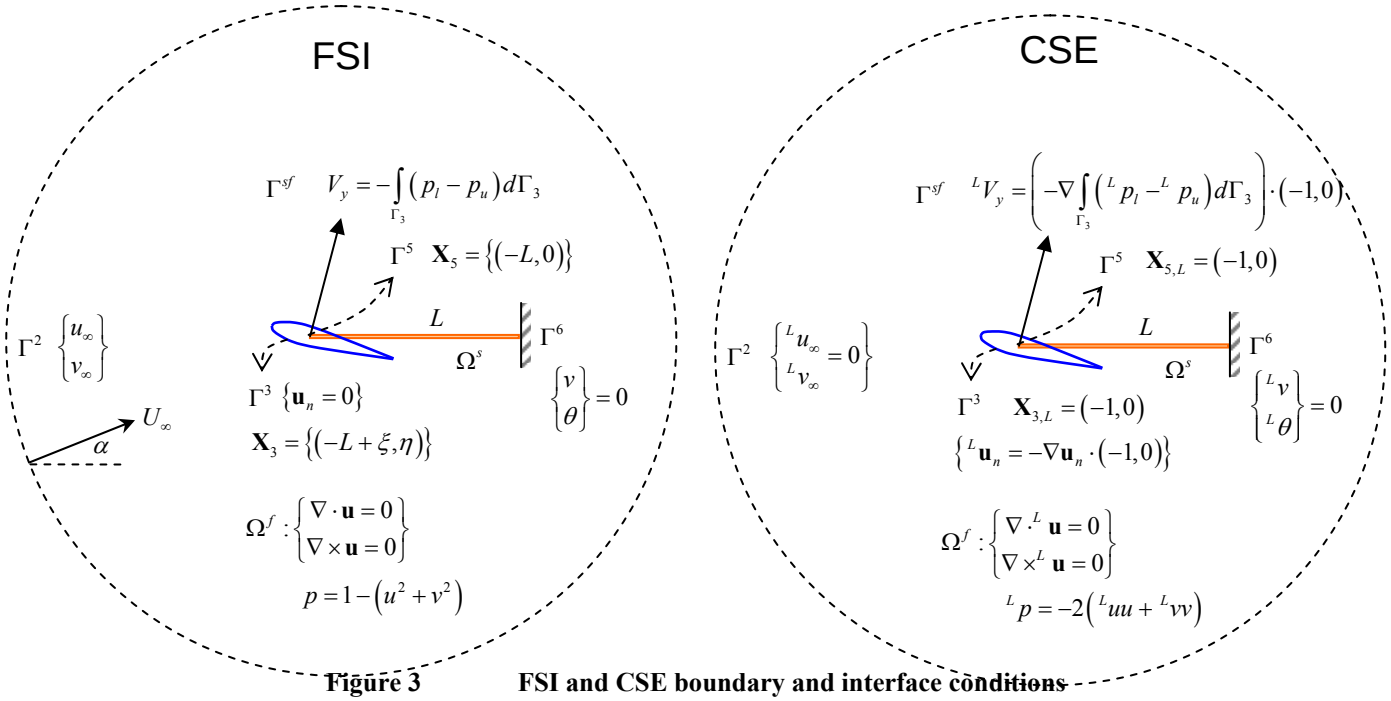

Figure 3 FSI and CSE boundary and interface conditions

Table 1 FSI problem boundary conditions

Boundary	Constrained dofs	
Freestream $\left(\Gamma^2\right)$	$u = U_\infty \cos\alpha \quad v = U_\infty \sin\alpha$	freestream conditions
airfoil surface $\left(\Gamma^3\right)$	$u_n = 0$	no penetration
beam tip $\left(\Gamma^{sf}\right)$	$V_y^s = -\int_{\Gamma_3} \left(p_l^f - p_u^f\right) d\Gamma_3$	fluid-structure interface (force equilibrium)
beam root $\left(\Gamma^6\right)$	$v = 0 \quad \theta = 0$	clamped

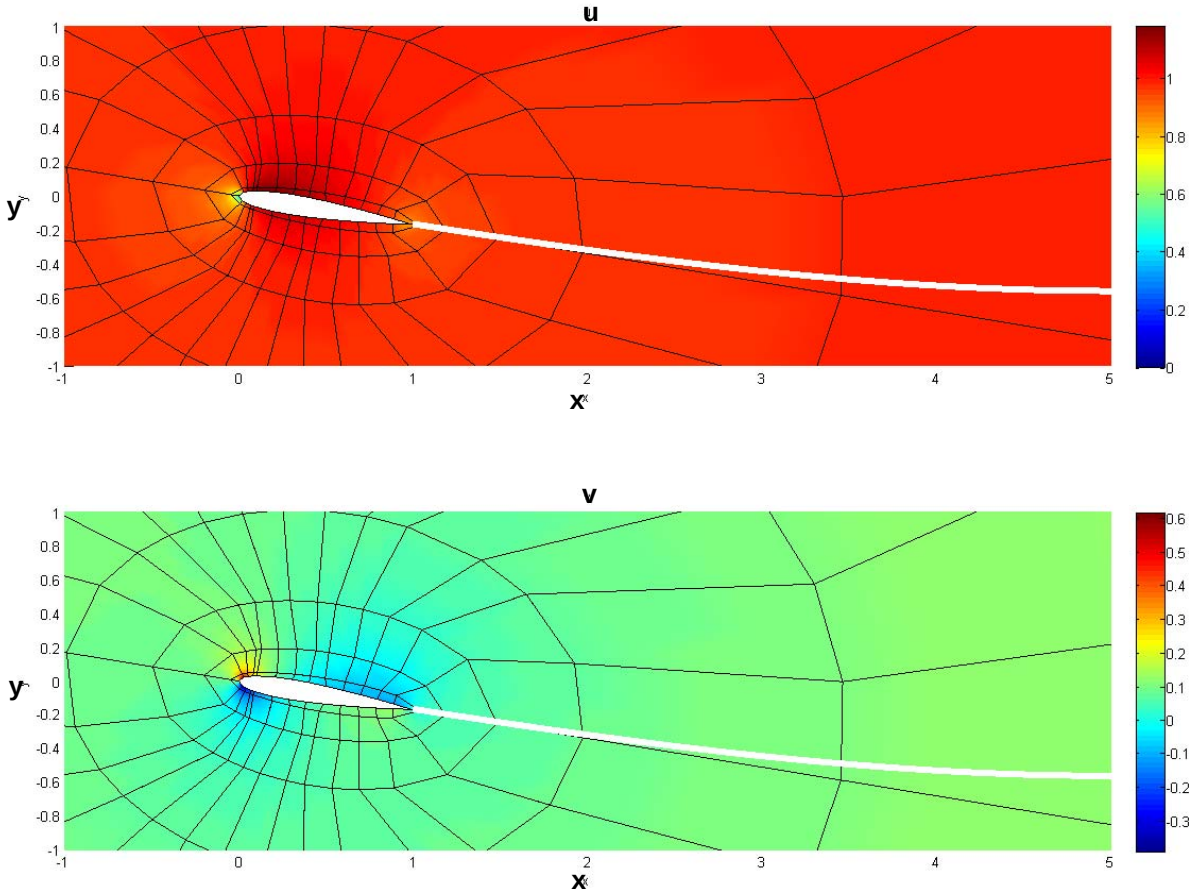

Figure 4 LSFEM FSI solution showing beam deflection (Fluid p = 4, Beam p = 4)

The solution gradients required for the CSE boundary conditions are determined by taking derivatives of the shape functions. Taking the sting length as the shape design parameter, we compute the sensitivity of the fluid domain flow and the beam deflection and rotation to the sting length. The beam coordinates are parameterized as the Cartesian ordered pair

$$\mathbf{X}_{\Omega^s} = \left\{ \left(\left[1 - \xi \right] L, \quad 0 \right) \middle| \, \xi \in \left[0,1 \right] \right\} \tag{40}$$

where L is the length of the sting. Similarly, the airfoil coordinates are parameterized as

$$\mathbf{X}_3 = \left\{ \left(-L + \xi, \eta \right) \middle| \, \xi, \eta \in \left[\mathbf{X}_{NACA\ 0012} \right] \right\} \tag{41}$$

Differentiating with respect to L defines the boundary shape sensitivity required for the advection term in (12). Thus, the airfoil boundary sensitivity to sting length is

$$\frac{\partial}{\partial L} \mathbf{X}_3 = \left\{ \begin{pmatrix} -1 & 0 \end{pmatrix} \right\} \tag{42}$$

which matches the shape sensitivity of the beam tip boundary. Since the airfoil surface remains a non-penetrating slip wall with variations in L, the airfoil surface CSE boundary condition reduce

$$\begin{Bmatrix} {}^{L}u^{f} \\ {}^{L}v^{f} \end{Bmatrix} = 0 - \begin{Bmatrix} \nabla u^{f} \\ \nabla v^{f} \end{Bmatrix} \cdot \frac{\partial \mathbf{X}_3}{\partial L} = \begin{Bmatrix} u^{f}_{,x} \\ v^{f}_{,x} \end{Bmatrix} \tag{43}$$

These values are determined from the LSFEM solution to the FSI problem and are plotted in Figure 5 . Enforcement of the CSE boundary conditions is done weakly through a boundary operator system, (2).

Following the sequential solution strategy used for the original FSI system, pressure sensitivity is calculated from the flow sensitivity solution. The pressure sensitivity

$$ {}^{L}p = -2\left({}^{L}u u + {}^{L}v v \right) \tag{44} $$

is a function of both the original flow solution and the sensitivity flow solution and is determined by differentiating (17). Due to the symmetry of the airfoil, the airfoil does not transmit a moment at the tip of the beam. No other boundaries are affected by a variation of the sting length and thus the remaining CSE boundary conditions are homogenous.

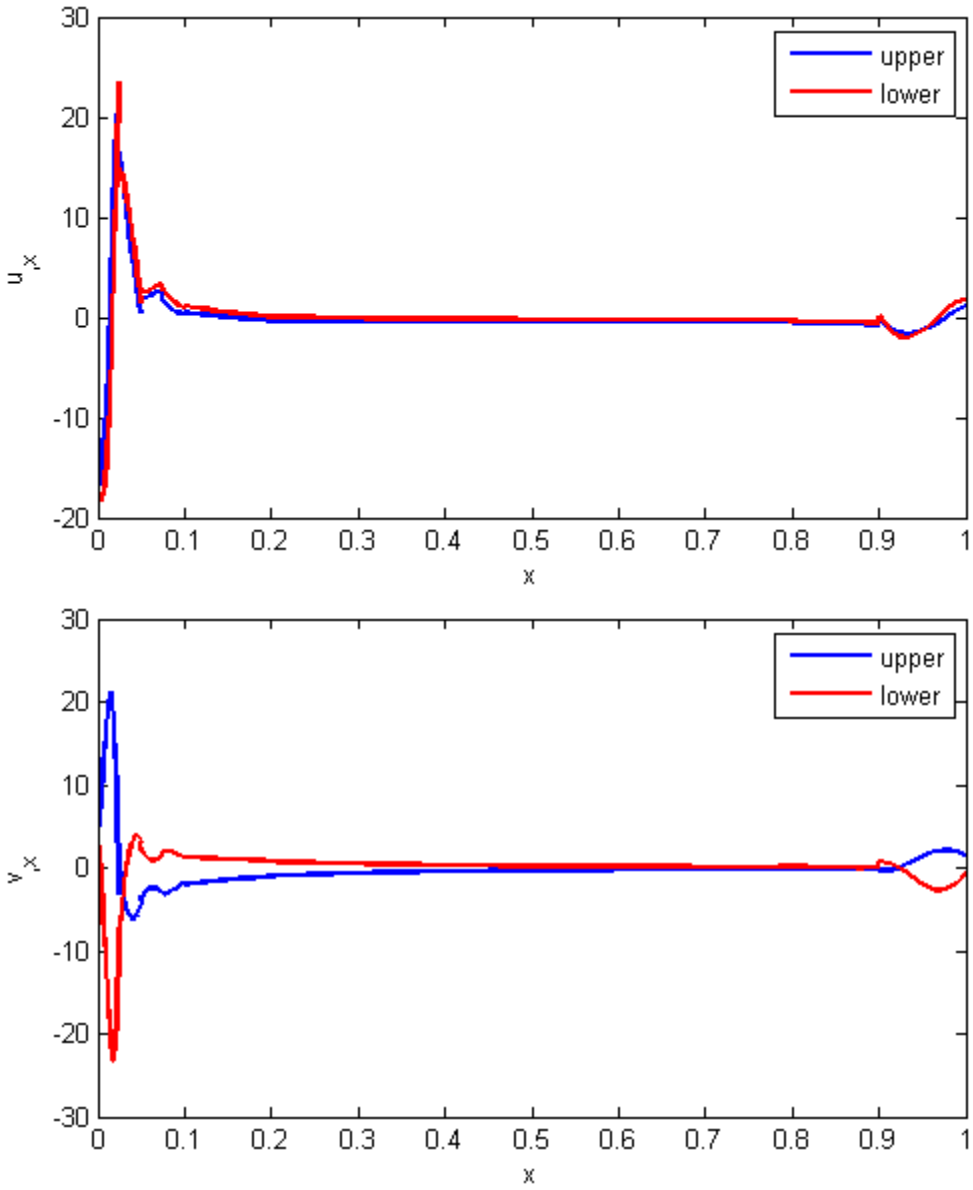

Figure 5 Airfoil surface flow sensitivity boundary conditions

The least-squares CSE flow solution is given in Figure 6 . The airfoil coordinates shift left with increasing sting length and, as expected, the flow solution shows the greatest sensitivity at the leading edge of the airfoil. The beam deflection and rotation sensitivity is compared to sensitivity obtained by finite difference methods in Figure 7 . Finite difference methods by nature give the total material derivative, (11). By definition, the continuous sensitivity variables represent the local derivative (Eulerian point). The CSE total material derivative may be calculated by

adding the advection term in (11) generated from the original system solution to the local CSE derivative obtained by solving the CSE system. Both the CSE local and CSE total derivatives are plotted in Figure 7 . The CSE total and finite difference derivatives for deflection sensitivity match exactly throughout the structure domain. The match is also exact for rotation sensitivity for the right half of the sting, though there is a small discrepancy between the CSE and finite difference sensitivities towards the beam tip.

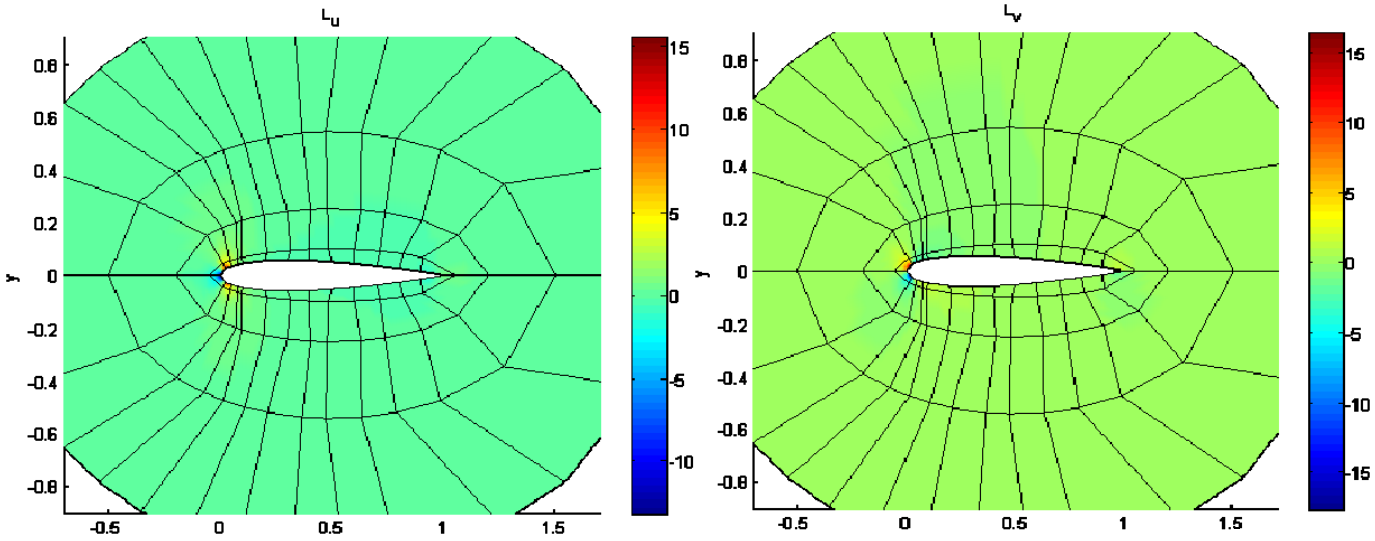

Figure 6 **Least-squares continuous sensitivity solution (p = 8) for flow variables**

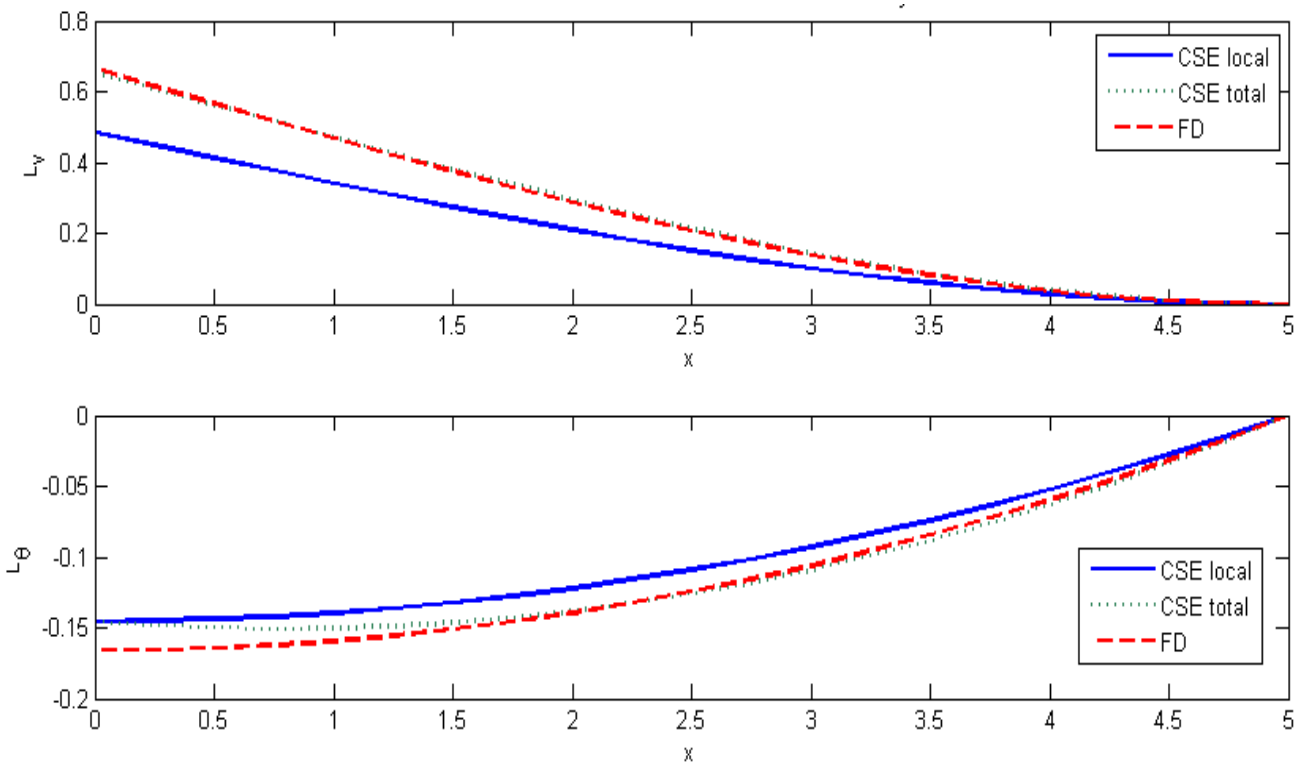

Figure 7 **Least-squares continuous and finite difference sensitivity for beam deflection and rotation**

The original FSI problem was solved using a *p*-value of 4 for both the fluid and structure domains. A *p*-convergence study for this problem dictated that a minimum a *p*-value of 8 for the fluid domain (a three-fold increase in the fluid degrees of freedom) was needed for good results. An examination of the element residual plot for the CSE system indicated that the mesh is far from optimally graded, nevertheless, the need for a more refined solution to the CSE equations is an observation previously made with regard to other systems [8]. It is convenient to use the same mesh for both the original system and the sensitivity system and to obtain the more refined solution through higher order *p*-elements. This is a distinct advantage of higher-order FEM since *p*-refinement allows a straightforward means to achieve a refined solution without needing a refined mesh.

VI. Conclusion

A least-squares continuous sensitivity analysis method was developed for fluid-structure interaction problems. LSFEM was used to solve both a sequentially-coupled fluid-structure system and the continuous sensitivity system. Gradients of the LSFEM solution and boundary conditions permitted a straightforward method for specifying the CSE boundary conditions. An example fluid-structure interaction problem was solved and the results were compared to finite difference sensitivities. The CSE equations required a higher *p*-value than the original system, a result previously observed. The higher-order least-square method employed permitted a straightforward method for CSE solution refinement on the same original computational mesh. Overall, the least-squares, continuous sensitivity analysis approach appears promising and should be applicable to more complicated, transient, nonlinear fluid-structure interaction problems.

VII. Acknowledgements

The Air Force Office of Scientific Research (AFOSR) and the Air Force Research Laboratory (AFRL) Air Vehicles Directorate funded this research. The authors gratefully acknowledge the support of AFOSR program manager Dr. Fariba Fahroo and the AFRL Senior Aerospace Engineers Dr. Raymond Kolonay, Dr. Phillip Beran, and Dr. Maxwell Blair.

VIII. References

[1] Rasmussen, C., Canfield, R., and and Reddy, J.N., "Nonlinear Transient Gust Response Using a Fully- Coupled Least- Squares Finite Element Formulation," Vol. AIAA-2008-1821, 2008,

[2] Roberts, R.W., and Canfield, R.A., "
Enriched Multipoint Cubic Approximations for Large-Scale Optimization," Vol. AIAA-2008-2146, 2008,

[3] Haug, E.J., Choi, K.K., and Komkov, V., "Design sensitivity analysis of structural systems," *Mathematics in science and engineering,* Vol. 177, Academic Press, Orlando, 1986, pp. 381.

[4] Choi, K.K., and Kim, N.H., "Structural sensitivity analysis and optimization," *Mechanical engineering series,* Springer Science+Business Media, New York, 2005,

[5] Borggaard, J., and Burns, J., "A Sensitivity Equation Approach to Shape Optimization in FLuid Flows," Langley Research Center, NASA Contractor Report 191598 (ICASE Report No. 94-8), 1994.

[6] Borggaard, J., and Burns, J., "A PDE Sensitivity Equation Method for Optimal Aerodynamic Design," *Journal of Computational Physics,* Vol. 136, 1997, pp. 366--384.

[7] Haftka, R.T., and Gürdal, Z., "Elements of structural optimization," *Solid mechanics and its applications,* Vol. 11, Kluwer Academic Publishers, Dordrecht ; Boston, 1992, pp. 481.

[8] Stanley, L.G.D., and Stewart, D.L., "Design sensitivity analysis : computational issues of sensitivity equation methods," *Frontiers in applied mathematics,* Society for Industrial and Applied Mathematics, Philadelphia, 2002, pp. 139.

[9] Dems, K., and Haftka, R.T., "Two Approaches to Sensitivity Analysis for Shape Variation of Structures," *Mech. Struct. & Mach.,* Vol. 16, No. 4, 1988-1989, pp. 501-501-522.

[10] Arora, J.S., Lee, T.H., and Cardoso, J.B., "Structural Shape Design Sensitivity Analysis: A Unified Viewpoint," *AIAA-91-1214-CP,* 1991, pp. 675-675-683.

[11] Lund,E. (Institute of Mechanical Engineering, Aalborg University), "Shape design optimization of steady fluid-structure interaction problems with large displacements," *Collection of Technical Papers - AIAA/ASME/ASCE/AHS/ASC Structures, Structural Dynamics and Materials Conference,* Vol. 5, 2001, pp. 3241.

[12] Etienne, S., Hay, A., Garon, A., "Shape Sensitivity Analysis of Fluid-Structure Interaction Problems," AIAA, 2006,
[13] Etienne, S., Hay, A., Garon, A., "Sensitivity Analysis of Unsteady Fluid-Structure Interaction Problems," AIAA, 2007,
[14] Newsome, R.W., Berkooz, G., and Bhaskaran, R., "Use of Analytic Flow Sensitivities in Static Aeroelasticity," *AIAA Journal,* Vol. 36, No. 8, 1998, pp. 1537-1537-1540.
[15] Livne, E., "Future of Airplane Aeroelasticity," *Journal of Aircraft,* Vol. 40, No. 6, 2003, pp. 1066--1092.
[16] Bendiksen, O.O., "Modern developments in computational aeroelasticity," *Journal of Aerospace Engineering,* Vol. 218, 2004, pp. 157.
[17] Hubner, B., Walhorn, E., and Dinkler, D., "A monolithic approach to fluid–structure interaction using space–time finite elements," *Computer Methods in Applied Mechanics and Engineering,* 2004,
[18] Etienne,S. (Ecole Polytechnique de Montreal), "A monolithic formulation for unsteady Fluid-structure Interactions," *Collection of Technical Papers - 44th AIAA Aerospace Sciences Meeting, Collection of Technical Papers - 44th AIAA Aerospace Sciences Meeting,* Vol. 11, 2006, pp. 8301.
[19] Walhorn, E., Kölke, A., Hübner, B., "*Fluid-structure coupling within a monolithic model involving free surface flows*," *Computers and Structures,* Vol. 83, 2005, pp. 2100-2111.
[20] Heys, J.J., Manteuffel, T.A., McCormick, S.F., "First-order system least squares (FOSLS) for coupled fluid-elastic problems," *Journal of Computational Physics,* Vol. 195, No. 2, 2004, pp. 560-575.
[21] Bathe, K., and Zhang, h., "Finite element developments for general fluid flows with structural interactions," *International Journal for Numerical Methods in Engineering,* Vol. 60, 2004, pp. 213-213-232.
[22] Bathe, K., and Shanhong, H.Z., "Finite element analysis of fluid flows fully coupled with structural interactions," *Computer and Structures,* Vol. 72, 1999, pp. 1-1-16.
[23] Kayser-Herold, O., and Matthies, H.G., "A Unified Least-Squares Formulation for Fluid-Structure Interaction Problems," *Computer and Structures,* Vol. 85, 2007, pp. 998-998-1011.
[24] Rasmussen, C.C., Canfield, R.A., and Reddy, J.N., "The Least-Squares Finite Element Method Applied to Fluid-Structure Interaction Problems," AIAA, 2007,
[25] Bochev, P.B., and Gunzburger, M.D., "Finite Element Methods of Least-Squares Type," *SIAM Review,* Vol. 40, No. 4, 1998, pp. 789--837.
[26] Jiang, B., "The least-squares finite element method : theory and applications in computational fluid dynamics and electromagnetics," *Scientific computation,* Springer, Berlin ; New York, 1998, pp. 418.
[27] Yang, S., and Liu, J., "Analysis of Least Squares Finite Element Methods for A Parameter-Dependent First-Order System," *Numerical Functional Analysis and Optimization,* Vol. 19, 1998, pp. 191-213.
[28] Bramble, J.H., Lazarov, R.D., and Pasciak, J.E., "
Least-squares methods for linear elasticity based on a discrete minus one inner product." *Comput. Methods Appl. Mech. Engrg.,* Vol. 152, 2001, pp. 520--543.
[29] Proot, M. M. J., "The least-squares spectral element method: theory, implementation and application to incompressible flows," 2003,
[30] Cai, Z., Manteuffel, T., McCormick, S., " *First-order system least squares for the Stokes equations, with application to linear elasticity*," *SIAM Journal of Numerical Analysis,* Vol. 34, No. 5, 1997, pp. 1727--1741.
[31] Pontaza, J.P., "Least-squares variational principles and the finite element method: theory, formulations, and models for solid and fluid mechanics," *Finite Elements in Analysis and Design,* Vol. 41, No. 7-8, 2005, pp. 703.
[32] Pontaza, J.P., "Least-squares finite element formulation for shear-deformable shells," *Computer Methods in Applied Mechanics and Engineering,* Vol. 194, No. 21-24, 2005, pp. 2464.
[33] Kayser-Herold, O., and Matthies, H.G., "Least-Squares FEM Literature Review," Institute of Scientific Computing Technical University Braunschweig, 2005-05, Brunswick, Germany, 2005.
[34] Blair, M., Canfield, R.A., and Roberts, R., "A Joined-Wing Aeroelastic Design with Geometric Non-Linearity," *Journal of Aircraft,* Vol. 42, No. 4, 2005, pp. 832-832–848.
[35] Demasi, L., and Livne, E., "Exploratory Studies of Joined Wing Aeroelasticity," AIAA, 2005,
[36] Wickert, D.P., "Least-Squares, Continuous Sensitivity Analysis Methods For Nonlinear Fluid-Structure Interaction Problems
" 2009,
[37] Hodges, D.H., and Pierce, G.A., "Introduction to structural dynamics and aeroelasticity," *Cambridge aerospace series,* Vol. 15, Cambridge University Press, Cambridge, England ; New York, 2002, pp. 170.
[38] Gel'fand, I.M., Fomin, S.V., and Silverman, R.A., "Calculus of variations," Dover Publications, Mineola, N.Y., 2000, pp. 232.

[39] Reddy, J.N., "An introduction to the finite element method," *McGraw-Hill series in mechanical engineering,* McGraw-Hill Higher Education, New York, NY, 2006, pp. 766.
[40] Naylor, A.W., and Sell, G.R., "Linear operator theory in engineering and science," *Applied mathematical sciences,* Vol. 40, Springer-Verlag, New York, 1982, pp. 624.
[41] Cook, R.D., Malkus, D.S., and Plesha, M.E., "Concepts and applications of finite element analysis," Wiley, New York, 1989, pp. 630.
[42] Šolin, P., Segeth, K., and Doležel, I., "Higher-order finite element methods," *Studies in advanced mathematics,* Chapman & Hall/CRC, Boca Raton, FL, 2004, pp. 382.
[43] Szabo, B.A., and Babuška, I., "Finite element analysis," Wiley, New York, 1991, pp. 368.
[44] Karniadakis, G., and Sherwin, S.J., "Spectralhp element methods for computational fluid dynamics," *Numerical mathematics and scientific computation,* Oxford University Press, New York, 2005, pp. 657.